



ISSN: 2350-0328

**International Journal of Advanced Research in Science,
Engineering and Technology**

Vol. 6, Issue 4, April 2019

Effect of sodium hydroxide concentration of Plasma Anodic Oxidation on the properties of oxide film formed on AZ91D Magnesium Alloy

Sung-Hyung Lee*, Hitoshi Yashiro, Song-Zhu Kure-Chu

Gakkōhōjin Kitaharagakuen, Hirakawa 036-0146 Japan and Department of Chemistry and Biological Science, Iwate University, Morioka, Iwate 020-8551 Japan

Department of Chemistry and Biological Science, Iwate University, Morioka, Iwate 020-8551 Japan
Materials Function and Design, Nagoya Institute of Technology, Nagoya, Aichi 466-8555 Japan

ABSTRACT: This study optimizes the plasma anodizing process for AZ91D casting. We evaluate thickness, composition pore formation, surface roughness, and corrosion resistance of oxide films. As the concentration of the NaOH (Sodium hydroxide) increased, the surface roughness decreases, the oxide thickness decreases, and the corrosion resistance improves. Our results show that as the NaOH concentration increased from 0.06 M to 0.13 M and 0.25 M, the thickness of the oxide layer decreases and the surface roughness (Ra) decreases from 0.52 to 0.08 and 0.06 μm . Corrosion resistance increased from (RN) 6 to 8 and 9. As the concentration of the NaOH increased, the oxide of the magnesium component in the oxide film increased and the oxygen component decreased.

KEYWORDS: AZ91D Mg alloy, Plasma anodizing, Coating, Corrosion, Surface roughness, Thin films, Concentration, PEO

I. INTRODUCTION

Plasma anodization has been known since the 19th century, and has been gradually improved in Russia, Europe, and the United States.

The corrosion resistance of the surface of Mg alloys is low and its use is limited [Ref 1]. Mg alloys are lightweight and have attractive properties in strength, thermal conductivity, electrical conductivity and electromagnetic interference shielding ability. However, if the surface is not properly treated, the use of Mg alloys is crucially limited by its unique chemical activity. Accordingly, various surface treatment methods have been applied to solve the problems of Mg alloys.

Among them, plasma anodizing treatment is one of the most effective protection of the surface [Ref 1-7].

The objective of our series of studies [Ref 2,3] is to find the optimum condition in forming a better oxide film through the plasma anodizing process for AZ91D magnesium alloy. In this study, concentration control of the NaOH in single-pulse mode has been attempted to understand the effect of these parameters on the properties of the forming oxide film.

II. EXPERIMENTAL METHOD

As described in our earlier paper [Ref 2,3],

NaOH concentration changes of 0.13 M and 0.25 M sodium hydroxide were applied to a mixture of 2 g dm⁻³ sodium aluminate and 10 g dm⁻³ sodium silicate as the electrolyte solution. Due to heat generated during dielectric breakdown, the temperature of the electrolyte also increased over time. The temperature of the electrolyte solution was controlled using a stainless-steel heat exchanger. Cross-sections and compositions of the plasma anodized samples were observed by field emission scanning electron microscopy (FESEM) with elemental analysis (EDS). The surface roughness was measured using a surface roughness tester (MITUTOYO, SJ-400). Ra represents the average surface roughness value from the measurement centreline to the surface contour.

Electrochemical impedance spectroscopy (EIS) measurements were performed in a 3 mol dm⁻³ NaCl solution using a potentiostat/galvanostat (10V/2A, ZIVE SP2, WonATech, Co., Ltd) to evaluate corrosion characteristics. The frequency response analyser (FRA) was used to analyse the EIS output. Also, a salt spray test was conducted according to the American Society for Testing and Materials (ASTM)-B117 standard test using a 5 wt% NaCl solution maintained at 35 °C for 72 h using a salt spray tester.

III. RESULTS AND DISCUSSION

In order to investigate the influence of the NaOH concentration on the formation of the plasma oxide film, the pulse voltage was fixed at 150 V at 50 °C for 15 min, and the NaOH concentration was changed to 0.06 M, 0.13 M, and 0.25 M.

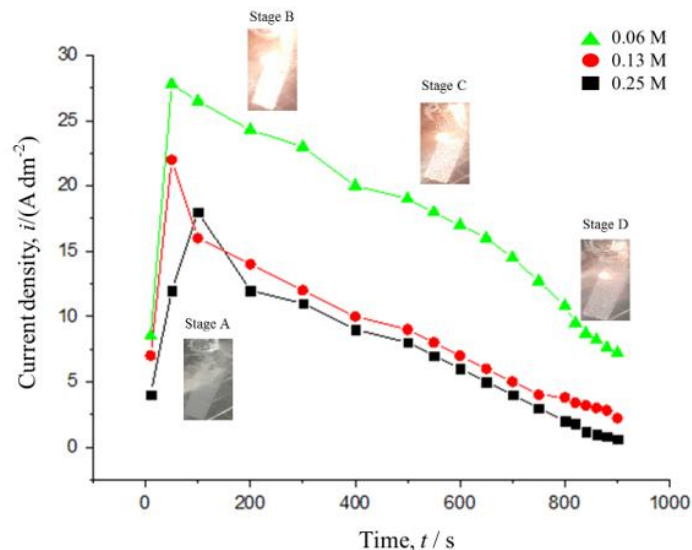


Figure 1. Typical variation of current density showing different stages of plasma anodization NaOH concentration at 50 °C.

Figure 1 shows the change in image and current of the plasma generated on the surface during the anodizing process. Plasma generation occurs through several steps, and other phenomena are also observed. Conventional anodization occurs at step A where significant gas evolution is observed. Voltage, threshold, breakdown voltage, and dielectric breakdown produce fine, uniform white microscale discharge at weak areas of the sample surface.

Over time, the amount of plasma generated on the surface increased. The maximum orange plasma volume was generated during step B-C, and in step D the volume occupied by plasma was increased [Ref 1-3].

The voltage response characteristics over time were similar at 0.06 M, 0.13 M and 0.25 M. However, when the NaOH concentration was low in the whole step, the voltage response was slightly slower.

An increase in electrolyte concentration is considered to be a good factor for the discharge channel and the plasma generation by increasing the electrolytic reaction of the electrolytic Mg alloy interface and increasing the mobility of the electrolyte solution. As the electrolyte concentration increased, the content of OH⁻ ions contained in the electrolyte increased, thereby increasing the electric conductivity of the electrolyte, thereby increasing the reaction with Mg + [Ref 8].

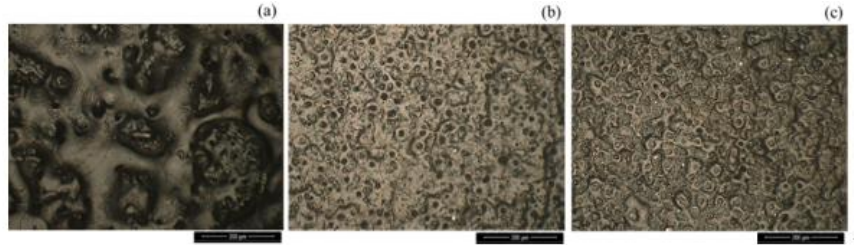


Figure 2. Digital microscope surface photographs at (a) 0.06 M, (b) 0.13 M, (c) 0.25 M.

Figure. 2 is an optical microscope image of the oxide film formed on the AZ91D material after plasma anodizing treatment, in which the concentration of the NaOH was changed to 0.06 M, 0.13 M, and 0.25 M at a fixed voltage of 150 V for 15 min. The surface of the oxide film formed in all samples contains crater traces, pores generated by secretions, and uneven products that generate craters. This phenomenon is caused by the plasma explosion of the surface of the sample at a high temperature at which molten Mg reacts rapidly with the NaOH and is cooled. We have found that the size of the pores produced by the plasma and the amount of product produced by the release decreases with increasing NaOH concentration.

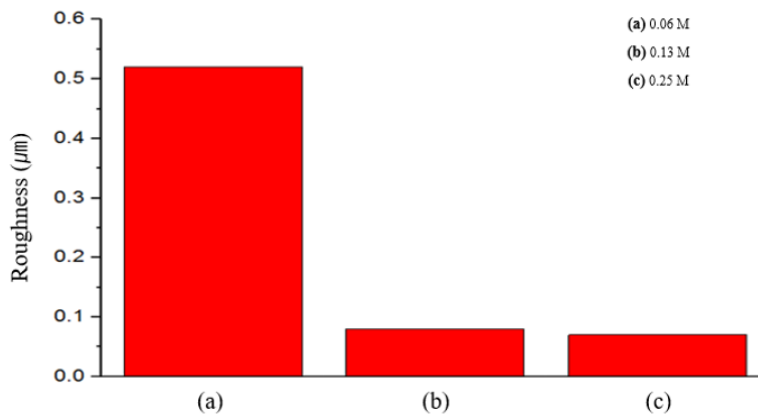


Figure 3. Surface roughness of the oxide film on the AZ91D surface after plasma anodization at (a) 0.06 M, (b) 0.13 M, (c) 0.25 M.

Figure 3 shows the roughness of the specimen with changes in NaOH concentration.

As the NaOH concentration increased from 0.06 M to 0.13 M and 0.25 M, the surface roughness decreased from 0.52 to 0.08 and 0.06 µm. The higher the concentration of the NaOH, the lower the surface roughness is.

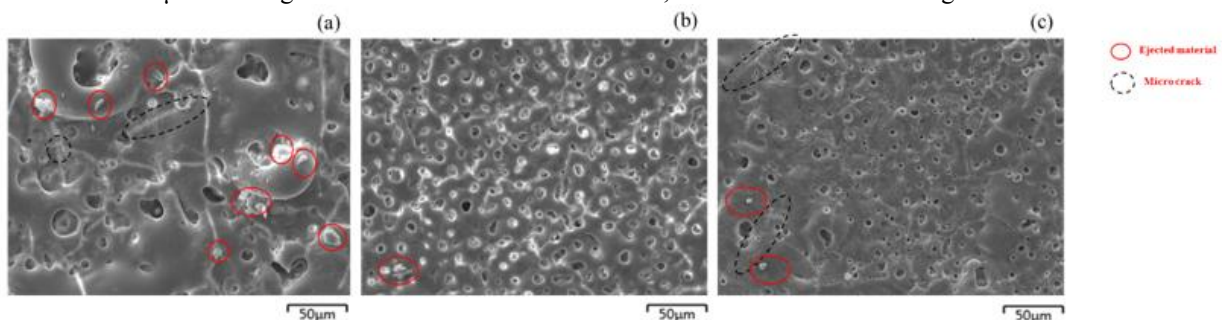


Figure 4. Surface morphologies of AZ91D after plasma anodization at (a) 0.06 M, (b) 0.13 M, (c) 0.25 M.

Figure 4 shows an FESEM image of a sample surface treated at 0.06 M, 0.13 M, and 0.25 M concentration of NaOH. The surface of the specimens treated at 0.06 M showed uneven porosity and some eject material and microcracks, which are holes created by the plasma at the material/oxide interface, leading to a porous coating with low durability [Ref 9].

The surface of oxidized specimens treated at 0.13 M and 0.25 M showed a relatively constant pore size and only a small amount of eject material was detected on the surface. Also, the number of eject material and microcracks was relatively small.

It is considered that the microcrack is caused by the fact that the tensile stress generated in the plasma electrolytic oxide film process becomes larger than the thermal expansion coefficient of the oxide film. The pores of the oxide film are generated by the generation of oxygen during the plasma anodizing process. Because the arc discharge time during the process is very short (about 10 μ s), the oxygen produced during the process is trapped in high-temperature and high-pressure molten oxides [Ref 10]. As the concentration of the electrolyte increased, the electrical conductivity of the electrolyte also increased. Increasing the electrical conductivity of the electrolyte lowers the breakdown voltage and reduces the dielectric strength during plasma anodization. Thus, the arc discharge forms a dense and uniform oxide film even if the plasma anode proceeds for the same time [Ref 11].

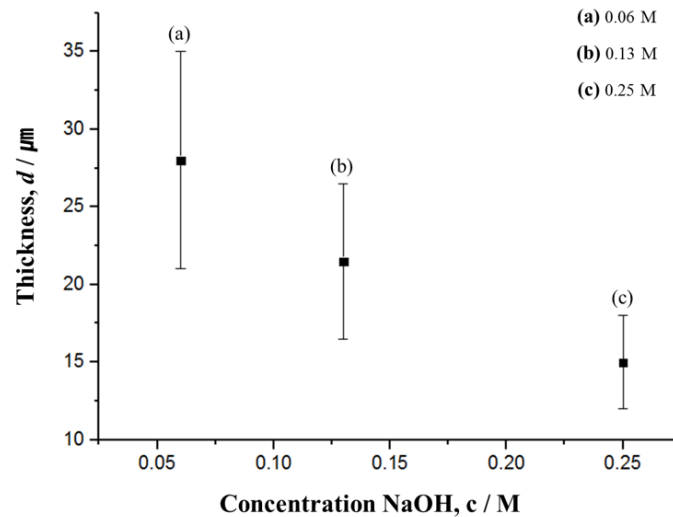


Figure 5. Oxide film thickness of AZ91D material formed by plasma anodization at (a) 0.06 M, (b) 0.13 M, (c) 0.25 M.

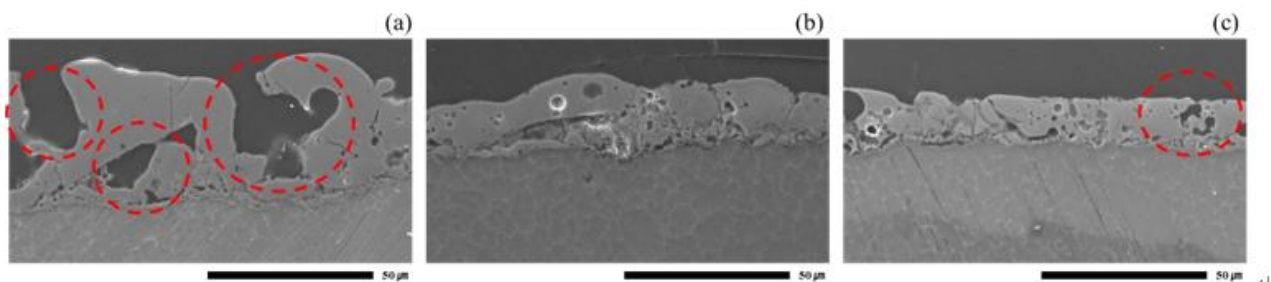


Figure 6. Cross-sectional view of AZ91D after plasma anodization at (a) 0.06 M, (b) 0.13 M, (c) 0.25 M.

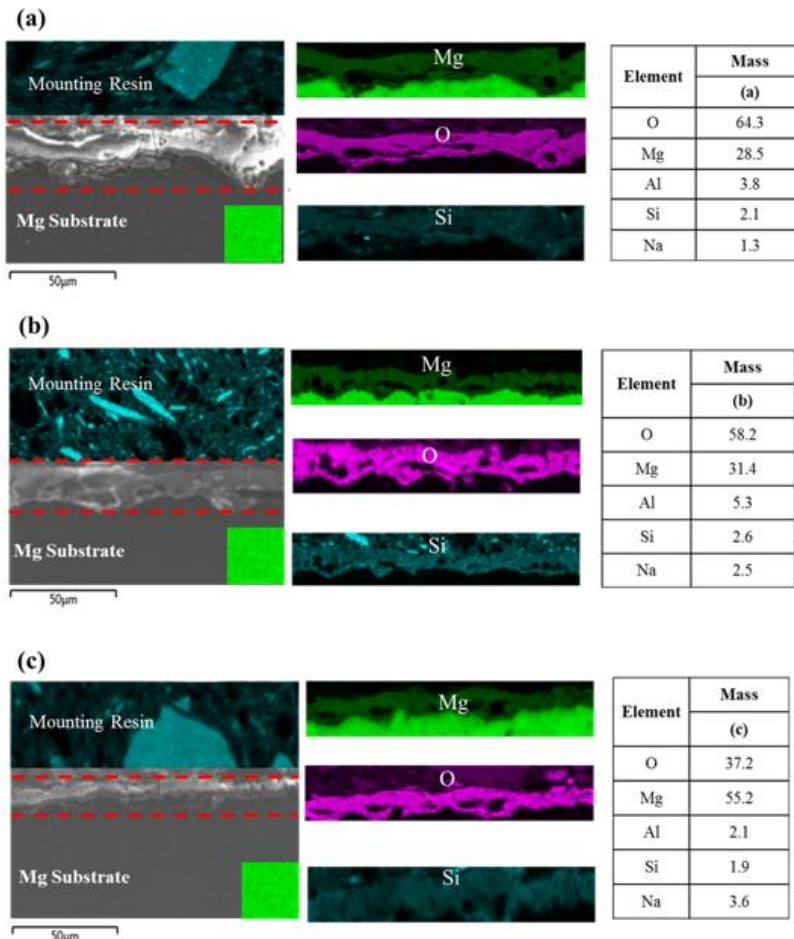


Figure 7. Cross sectional view of AZ91D after plasma anodizing at (a) 0.06 M, (b) 0.13 M, (c) 0.25 M.

Figures 5, 6 and 7 show the average film thickness, structure, and composition determined from the cross section of the 0.06–0.25 M plasma anodic oxide film.

Figures 5 and 6 show oxide film thickness and cross-sectional images. The thickness tends to decrease with increasing NaOH concentration. When the NaOH concentration was 0.06–0.25 M, the thickness of the oxide film was 21–35 µm, 16.5–22.5 µm, and 7–18 µm.

The plasma anodic oxide film had few defects and uniformly formed as the NaOH concentration increased, and the thickness was relatively low.

Figure 7 shows the EDS elemental mapping and distribution results for Mg, O and Si in the oxide film. Mg, O and Si were the main components of the film, and Si and O were uniformly distributed. As the concentration increased, Mg ions increased and oxygen decreased in mass. This can also explain the concentration dependence of the oxide thickness shown in Figures 6 and 7.

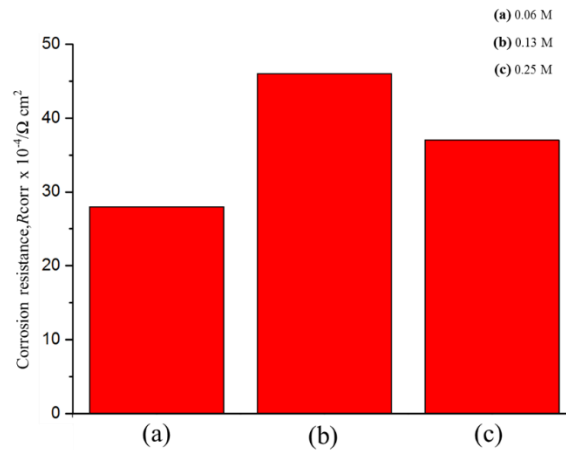


Figure 8. Effect of concentration on the corrosion resistance of AZ91D after plasma anodization (solution: 3 mol dm⁻³ NaCl, temperature: 25 °C).

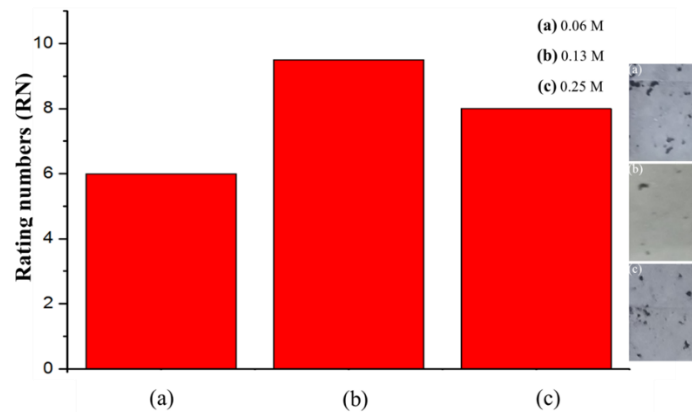


Figure 9. Surface images of specimens after the salt spray test (72 h).

Figure 8 shows the corrosion resistance measured in a 3 mol dm⁻³ NaCl solution using EIS as a function of solution temperature. As expected, an increase in the plasma-anodized NaOH concentration improves corrosion resistance, among which corrosion resistance is the best at a concentration of 0.13 M.

In this figure the corrosion resistance value is related to the magnitude of the AC impedance at 10 Hz.

Figure 9 shows the results of a brine spray test performed for 72 h in accordance with ASTM standards to evaluate the corrosion characteristics of plasma anodized Mg alloy specimens at various temperatures. The RN values were 0.06 M to 6 and the RN values of the anodized samples at 0.13–0.25 M were 9.5 and 8, respectively. These results demonstrate the effects of observed surface roughness, thickness, and trends in EIS data.

As the concentration of the NaOH increases, the thickness of the oxide film decreases. Figures 8 and 9 show that the corrosion resistance is improved as the concentration of the NaOH increases and is the best at a concentration of 0.13 M.

Generally, the thicker the coating layer in the coating process such as plating, the better the corrosion resistance. However, in the case of the oxide coating process, i.e., plasma anodization, the corrosion resistance is not proportional to the thickness of the oxide coating.

In this experiment, the temperature of the NaOH affects the arc discharge time and the arc strength as shown in the cross-sectional image of the oxide film in Fig. 7 and Fig. 8, and ultimately affects the oxide microstructure. As a result, when the test pieces are simultaneously treated at the same current density, the density of the oxide film becomes high when the concentration of the NaOH is high. High density oxide films significantly affect the corrosion resistance. The

porosity of the high density oxide film increases to lower the porosity and the oxide film having a low porosity cannot penetrate easily and the corrosion resistance is excellent.

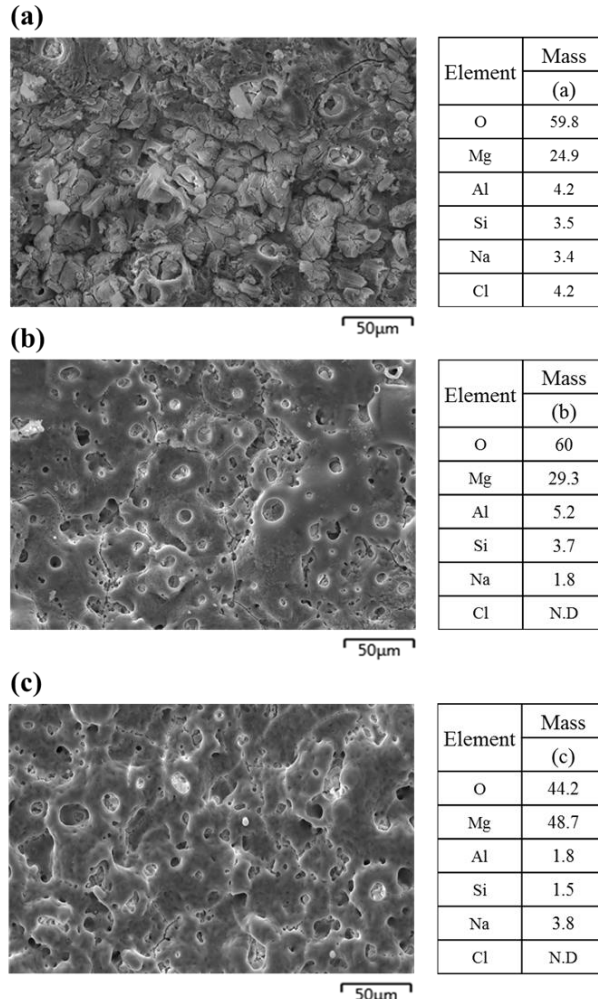


Figure 10. Surface micrograph of the corrosion area of AZ91 and EDS component analysis after the salt spray test 72 h, at (a) 0.06 M, (b) 0.13 M, (c) 0.25 M.

Figure 10 shows the surface and composition of the oxide film after the plasma anodized 72 h test at 0.06 M (a), 0.13 (b) and 0.25 M (c).

0.06 M (a) Aggressive Cl⁻ ions accumulate in the oxidized film cracks that have undergone corrosion, indicating that the entire oxide film is destroyed by Cl⁻ ions and the corrosion products spread on the upper surface of the oxide film and the protection of the oxide film is lost.

The corrosion reaction of Mg takes place through the following redox reaction:



Mg in a neutral or alkaline solution is oxidized to Mg²⁺ and reacts with OH⁻ ions formed by simultaneous reduction of water to form Mg(OH)₂ on the magnesium surface. The deteriorated surface roughness with more defects and pores at 0.06 M is therefore associated with lower durability of the material in a corrosive environment.

IV. CONCLUSION

We describe the plasma anodization procedure suitable for the anodization of Mg alloys and have demonstrated applicability to AZ91D alloys. The anodizing process is evaluated in relation to the NaOH concentration, and the



ISSN: 2350-0328

International Journal of Advanced Research in Science, Engineering and Technology

Vol. 6, Issue 4, April 2019

NaOH concentration can be optimized with a uniform oxide layer and better corrosion resistance. As the concentration of treated NaOH increased from 0.06 M to 0.13 M and 0.25 M, the surface roughness decreased, the thickness of the oxide film decreased, and the oxide film defect on the surface and the cross section also decreased.

The optimum NaOH concentration was 0.13 M and the corrosion resistance increased from $R_N = 6.0$ to 9.

Mg, Al, O and Si were uniformly distributed on the surface of the oxide films under optimized conditions. As the NaOH concentrations increased, the oxygen content in the oxide film decreased due to dehydration, and Cl⁻ ions were detected in the corroded area. Based on the results of this study, the NaOH concentration of 0.13 M is favorable for plasma anodizing of AZ91D, and a film with excellent homogeneity and corrosion resistance is obtained.

REFERENCES

- [1] Mordike, B. L., and Tü Ebert. "Magnesium: properties—applications—potential." *Materials Science and Engineering: A* 302.1 (2001): 37-45.
- [2] S.H. Lee, H. Yashiro and S.-Z. Kure-Chu, Fabrication of Plasma Electrolytic Oxidation Coatings on Magnesium AZ91D Casting Alloys, *J. Korean Inst. Surf. Eng.*, 2017, 50(6), p 432-438.
- [3] S.H. Lee, H. Yashiro and S.-Z. Kure-Chu, Effect of Power Mode of Plasma Anodization on the Properties of formed Oxide Films on AZ91D Magnesium Alloy. *Korean Journal of Materials Research*, 2018, 28.10: 544-550.
- [4] Song, Guangling, et al. "The electrochemical corrosion of pure magnesium in 1 N NaCl." *Corrosion Science* 39.5 (1997): 855-875.
- [5] Ma, Y., et al. "Systematic study of the electrolytic plasma oxidation process on a Mg alloy for corrosion protection." *Thin Solid Films* 494.1-2 (2006): 296-301.
- [6] Gray, JEL, and Ben Luan. "Protective coatings on magnesium and its alloys—a critical review." *Journal of alloys and compounds* 336.1-2 (2002): 88-113.
- [7] D. K. Lee, Y. H. Kim, H. Park, U. C. Jung, and W. S Chung, *Journal of Korea Institute Surface Engineering*, 42,3 (2009).
- [8] Moon, Sungmo, and Yunkyung Nam. "Anodic oxidation of Mg–Sn alloys in alkaline solutions." *Corrosion Science* 65 (2012): 494-501.
- [9] Atar, Erdem, et al. "Residual stress estimation of ceramic thin films by X-ray diffraction and indentation techniques." *ScriptaMaterialia* 48.9 (2003): 1331-1336.
- [10] Narayanan, TSN Sankara, Il Song Park, and Min Ho Lee. "Strategies to improve the corrosion resistance of microarc oxidation (MAO) coated magnesium alloys for degradable implants: Prospects and challenges." *Progress in Materials Science* 60 (2014): 1-71.
- [11] Srinivasan, P. Bala, C. Blawert, and W. Dietzel. "Effect of plasma electrolytic oxidation treatment on the corrosion and stress corrosion cracking behaviour of AM50 magnesium alloy." *Materials Science and Engineering: A* 494.1-2 (2008): 401-406.